A delta (function) in a river

Nicholas Tufillaro,* Philipp Grötsch, and Luke Zeitlin

Gybe, Corvallis, Oregon 97333 USA

(Dated: February 24, 2026)

Abstract

We examine a data set that follows a pulse of turbidity down the Klamath River on 27 November 2025. The basic theory and data analysis provides an environmentally relevant application of the utility of linear wave theory and illustrates how high-frequency gauging can be used to mimic tracer experiments to arrive at estimates of basic flow parameters such as disperson. In addition to reseachers, this paper could also be of interest to teachers looking for examples of the application of applied mathematics to environmental monitoring.

I. INTRODUCTION

Environmental monitoring generates massive streams of data, creating rich opportunities for research as well as training of undergraduates in the application of quantiative techniques to environmental sciences. As an example, we examine sediment transport in the Klamath River following the 2024 removal of four dams. The aim of removing the dams is to restore the watershed's ecology, particularly for native species such as Chinook and coho salmon.[1] We use high-frequency turbidity measurements from autonomous river gaging—courtesy of the Karuk and Yurok Tribes—to demonstrate how a delta function aids in estimating the transport of large sediment flushes ('slugs') down the river, the so-called 'routing problem'.[2] The delta function enters this story via solutions of the advection-dispersion equation.

The one-dimensional advection-dispersion equation (ADE) is usually the starting point for understanding how concentrations of sediments, nutrients, or other chemicals vary as they move down a river. The ADE contains two parameters: u [m/s], the longitudinal stream velocity, and D [m^2/s], the dispersion. Typically, these parameters are found through 'tracer' experiments.[3] A dye is released into the water at a fixed time and place, and downstream concentrations of the dye are measured. From this data, average values of u and D are estimated for different river sections. Once parameterized, the ADE can estimate transport. This includes scenarios such as the accidental release of a pollutant and its potential arrival downstream at a point of concern. As you might imagine, tracer experiments require significant effort to obtain information that is useful but limited in both space and time.

In recent years, open data sources of high-frequency river gauging, such as the USGS 'super gages' provide temporally dense (every 15 minutes) data on turbidity (which can often be used as a proxy for sediment concentrations[4]), nutrients, and other biogeochemical parameters.[5] In this paper, we illustrate how high-frequency gauging can be used to mimic tracer experiments. River flows are often separated into a 'base flow' and 'event flows.' An event flow can arise from storm runoff, leading to a wave packet (a slug) of high turbidity water moving coherently downstream. In the cases we look at here, the 'event' is due to a water release from dams as part of the dam removal process, or normal operations. The turbidity slug (or any other quantity such as a nutrient measured by high-frequency gauging) can serve as a tracer, potentially providing a tool for river modeling that offers much greater temporal and spatial coverage than tracer experiments alone.

The techniques needed for this type of river modeling are part of a many undergraduate's toolkit, ranging from a working knowledge of basic linear wave phenomena to, in more advanced classes, their solution via convolution integrals and Green's function. The delta function enters here with a kind of slippery issue. In the typical tracer experiment, the delta function is used to model the entrance of the tracer at a known place and time. However, with high-frequency gauging, the initial formation of a slug is more temporally and spatially complex. To mimic the standard tracer experiment, we would like to replace the actual slug formation with a useful fiction, a delta function (or sequence of functions) placed in the river such that it approximately reproduces the observed slug behavior downstream. The solution presented here is not unique and relies on a few plausible heuristics. The utility of the method can be evaluated by testing against high-frequency river gauging data from open data sources. We suspect there is a trove of cool problems in environmental monitoring that mix big data with simple physical models, opening new doors for interesting discoveries by keen undergraduates.

In Section 2 we provide site information about the Klamath River dam removal project. Section 3 describes the basics of the one-dimensional advection-dispersion equation, its fundamental solution via a delta function, and its application to river modeling. Section 4 presents a solution as to 'where to place a delta function in a river' to mimic the downstream gauging data, and Section 5 offers some concluding remarks.

II. THE KLAMATH RIVER: SITE INFORMATION

The Klamath River runs 408 km from its source at Klamath Lake in Southern Oregon to the Pacific Ocean at the town of Klamath in Northern California. The river flows through several native peoples' territories, specifically the Yurok tribe at its mouth and the Karuk tribe along their ancestral homelands. Four hydroelectric dams—J.C. Boyle, Copco No. 1, Copco No. 2, and Iron Gate—were built in the upper reach of the river between 1911 and 1962. They were breached and removed in 2024. Built for hydroelectric power, the dams were removed due to efforts led by native tribes to restore the watershed's ecological health. The dams blocked access to salmon spawning grounds, and caused massive toxic algae blooms in upstream reservoirs and created fluvial conditions that favored a myxozoan parasite responsible for juvenile salmonid fish kills.

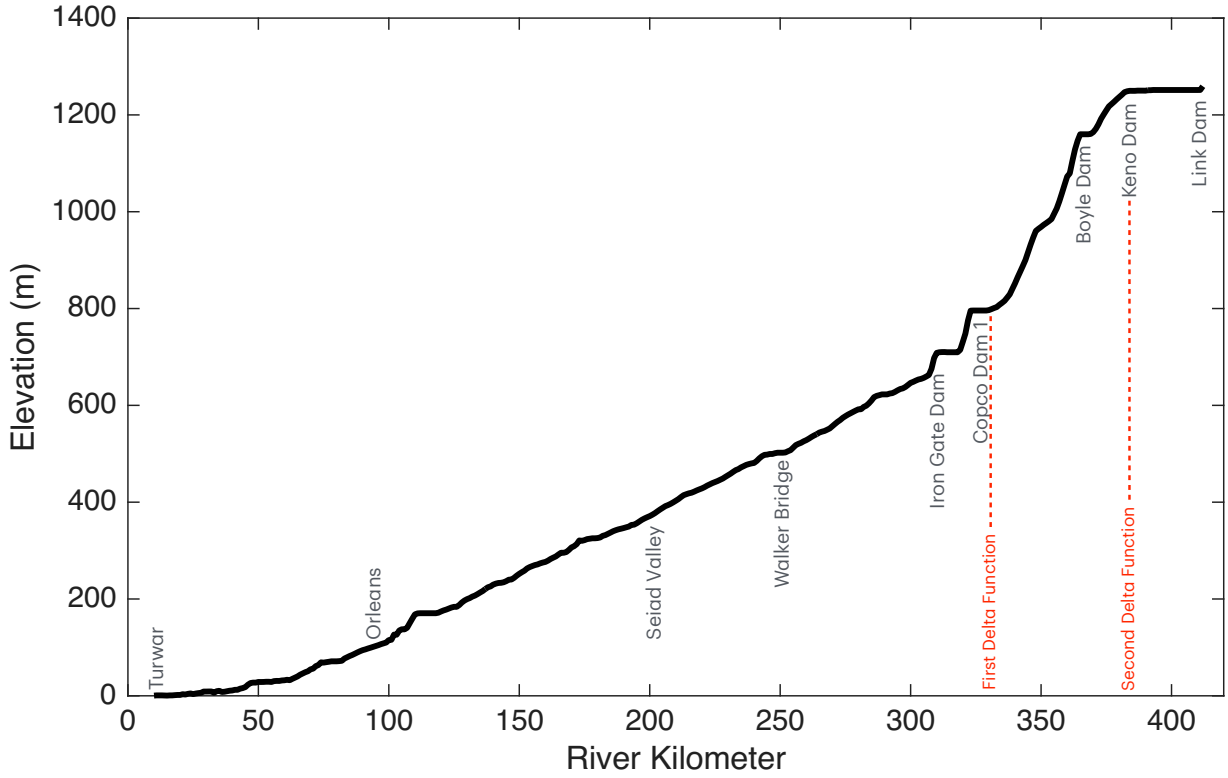

FIG. 1. Elevation map (pre-dam removal) for the Klamath River. Gauge locations are indicated along with the location of 'fictional' delta functions estimated in Section 4.

Dams have a limited lifetime, often about a century, because sediments build up behind them. Removing a dam causes large sediment flushes during the breach. Further sediment flushes occur through controlled releases from upstream dams. These releases are designed to help clear out accumulated sediments and restore the river channel. To monitor the river, the Karuk Tribe (Ref. 6) and the USGS (Ref. 7) installed a sequence of high-frequency water quality gauges, including turbidity measurements, along the Klamath River at locations indicated in Fig. 1, which presents an elevation map of the river, also indicating the location of the dams and gauges.

Turbidity is an empirical water quality parameter measured optically[8] that indicates water clarity. It can be linearly correlated with physical parameters like sediment concentrations using site-specific calibrations.[4] At the very top of the river reach (Fig. 1) are the

Keno and Link Dams, which were not removed. Controlled releases from these dams can result in sediment flushes, slugs (wave packets) propagating down the river. Sediment slugs can also result from intense rain events and the resultant storm run-off, which usually occurs along the US West Coast in the winter months.

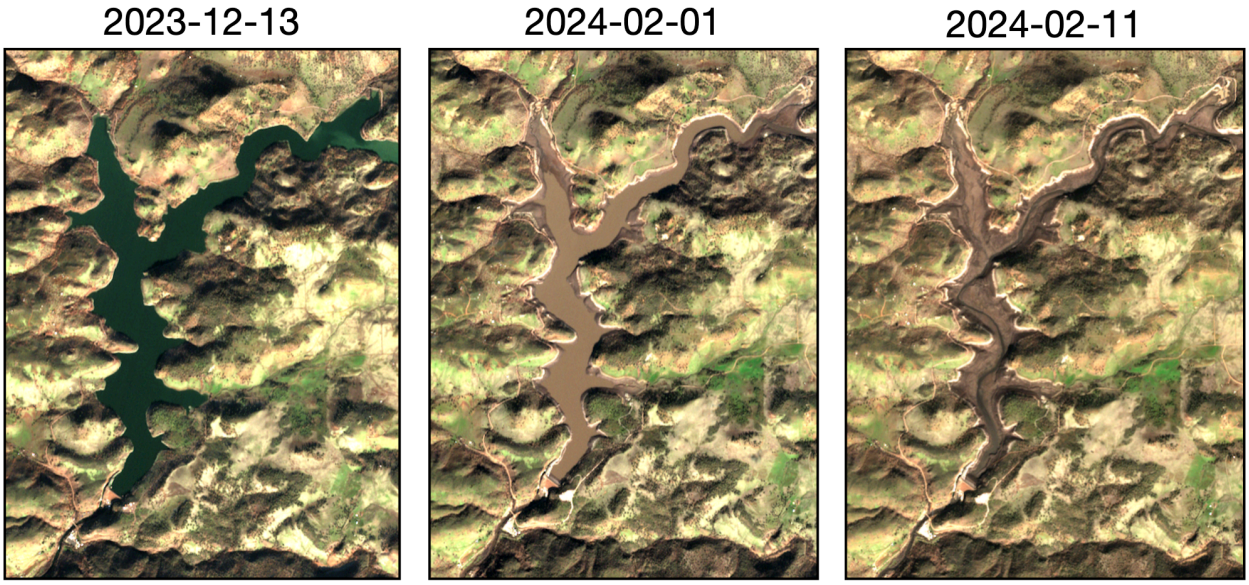

FIG. 2. Sentinel-2 imagery of Iron Gate Reservoir pre- and post-dam removal.

Iron Gate was the largest dam on the Klamath, and Fig. 2 shows remote sensing imagery of the reservoir right before, during, and after the dam breach in January 2024.[9] Note the high sediment loads visible in Fig. 2(b) during the dam removal period. As described in Section 4, the sediment released down the river produces slugs of turbidity whose basic outline is consistent with a description by the ADE equation. Figure 3 shows an example of the evolution of a turbidity slug generated by a controlled release at the Keno Dam on 27 February 2025 and illustrates several points.

The gauge data records the turbidity values every 15 minutes. In Fig. 3, the gauge data at each location are temporally aligned by the passage of the peak values and stacked on top of one another. The easternmost location is Iron Gate at 309 km upriver, and the westernmost location is the Turwar gauge, right before the estuary, 8 km upriver. The slug clearly disperses, as indicated by the systematic decrease in peak amplitude and the increase in pulse width, as it travels downstream. A base flow with turbidity values between 50-100 FNU also decreases as we head downstream. If we subtract this baseflow using linear interpolation, the remaining data closely resembles the data generated from a linear system's

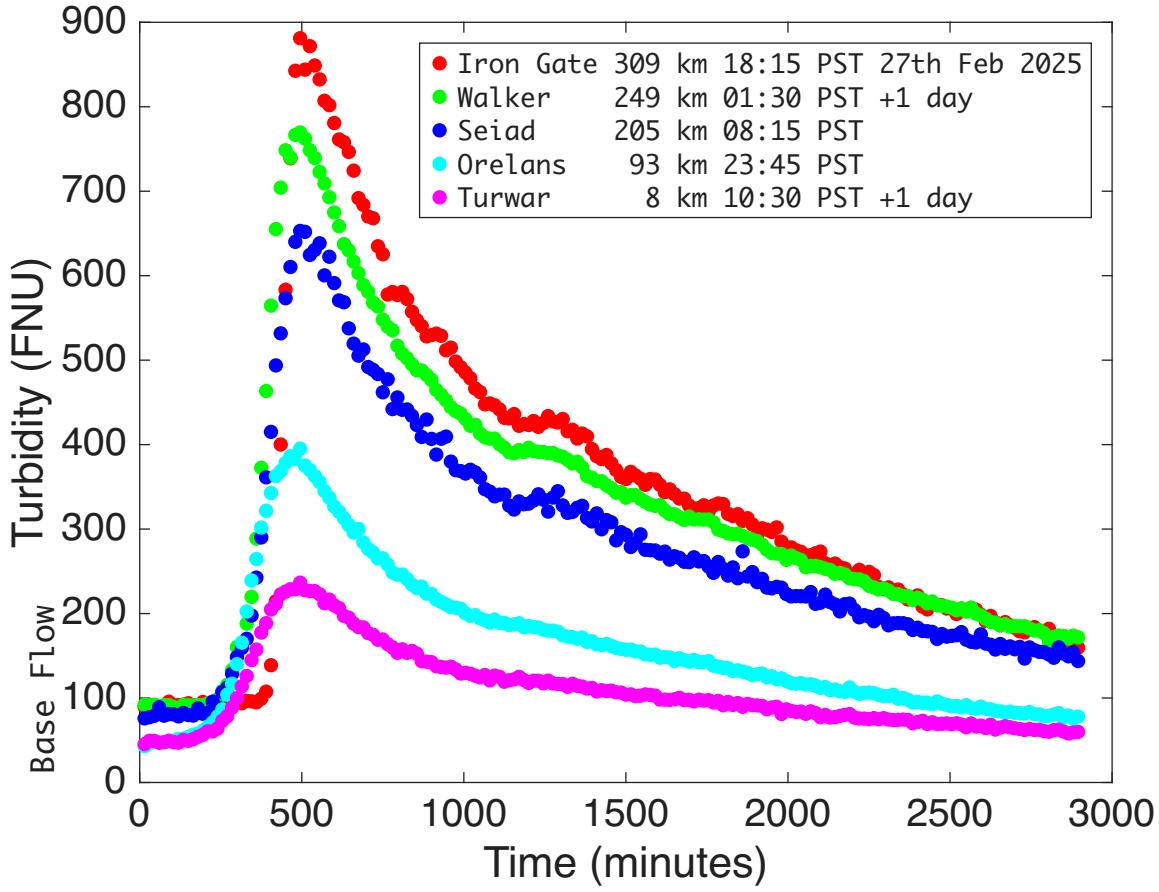

FIG. 3. Turbidity slug measurements after a controlled release from Keno Dam (385 km) starting on 27 Febuary 2025 show the pulse as it passes the stations indicated on Fig. 1. The sampling interval is 15 minutes, and the signals have been aligned and stacked by correlating the peaks. As the slug flows downstream the peak decreases, and width of the pulse increases. A base flow turbidity also decrease from $\approx$ 100 to 50 FNU as the pulse moves downstream. The pulse takes $\approx$ 40 hours to travel from Iron Gate (309 km) to the Estuary (0 km)

impulse-response test, which motivates the modeling approach described here.[10]

Such an impulse response approach to modeling sediment transport is well-known to river scientists as the 'routing-method' and is commonly used in tracer studies.[11] In a companion paper[12] we present results of this routing method for the whole Klamath River, but in this paper, we want to focus on transport along only the uppermost section, and how the release of water at the Keno Dam at 385 river km results in the formation of a highly peaked turbidity slug at 309 river km. More specifically, we ask the question of whether we can

place a 'delta function' in the river at a location above 308 river km to mimic the response we see experimentally in the gauge data at Iron Gate. There are many possible ways to do this, so the question becomes whether there is a principled or unique way to specify where to place the delta function. As mentioned, the use of the delta function in this manner is purely a fiction — like the delta function itself[13]— but the secondary question is, how useful is this fiction?

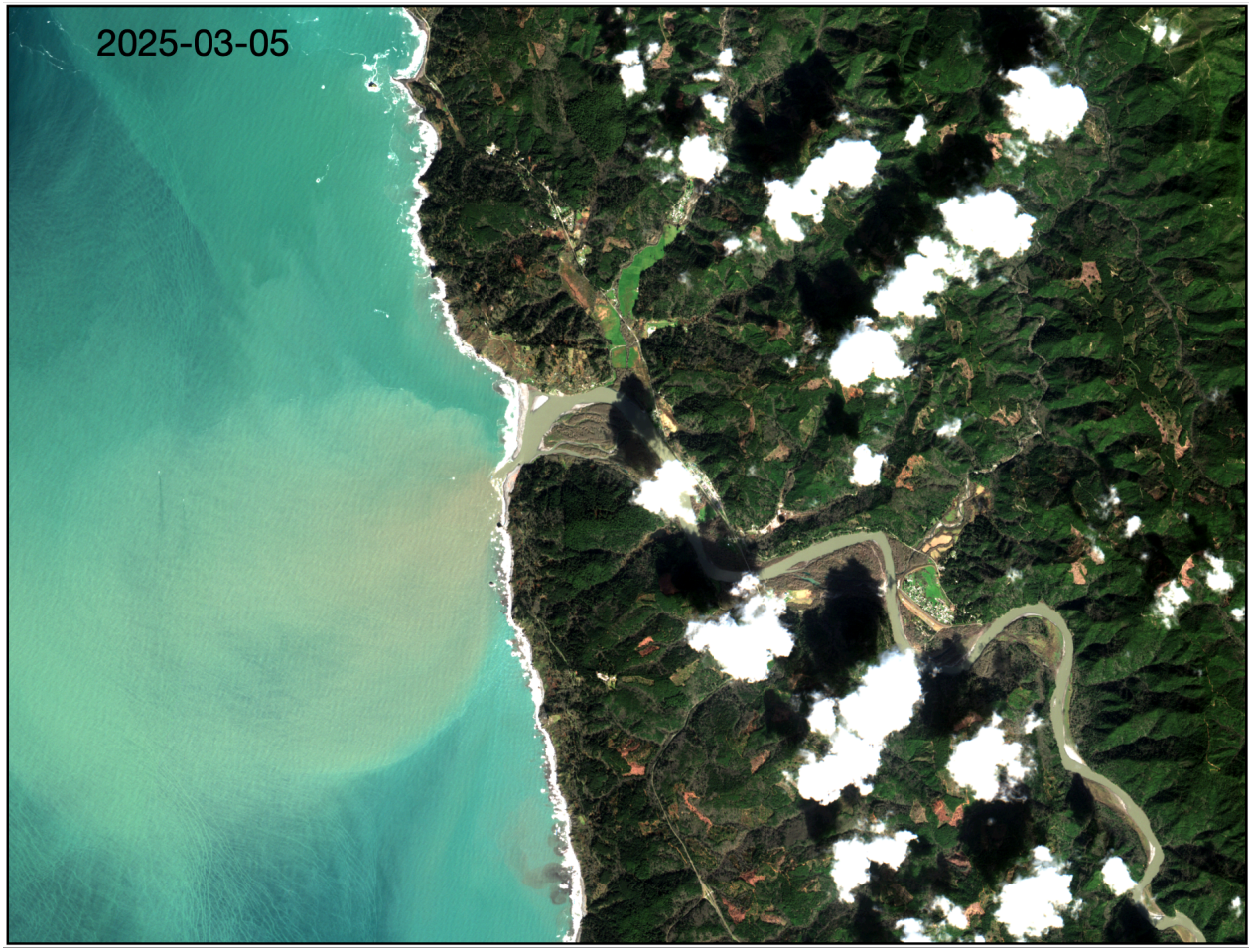

FIG. 4. Sentinel-2 image of the Klamath River plume entering the Pacific ocean on 5 March 2025 (11:19 PST) near the tail end of the turbidity pulse.

Table I summarizes a few details about the gauge data for the slug generated on 27 February 2025. In particular, an estimation of the average velocity based on the time of passage of turbidity peaks shows that the velocity starts at a very swift ≈ 7 m/s, and is still swift in the Iron Gate region at ≈ 3 m/s. Below Iron Gate — at Walker, Seiad, and Turwar – the average velocity is approximately 2 m/s, still quick by typical base flow standards

TABLE I. Gauge Station River Parameters

Station	River Km	Peak Arrival (PST)	Peak Turbitity (minus base)	Avg. Velocity (m/s)
Keno	385	2025-02-27 12:30	170	
Boyle	364	13:15	431	7.78
Iron Gate	309	18:15	881 (789)	3.06
Walker Bridge	249	2025-02-28 01:30	770 (672)	2.30
Seiad	205	08:15	653 (571)	1.81
Orleans	93	23:45	395 (352)	2.01
Turwar	8	2025-03-01 10:30	237 (196)	2.20

(< 1 m/s). These velocity values are consistent with the river elevation presented in Fig. 1. When the turbidity slug reaches the river's mouth, it generates a plume into the Pacific Ocean, visible in the satellite imagery shown in Fig. 4.

III. THE ADVECTION-DISPERSION EQUATION (ADE) AND ITS PRINCIPAL SOLUTION

The advection-dispersion equation is used to model many systems, including flows in a uniform channel, where it takes the form:

$$\frac{\partial C}{\partial t} = D\frac{\partial^2 C}{\partial x^2} - u\frac{\partial C}{\partial x} \tag{1}$$

C (typically [g/m^3]) is a cross-sectional average of the water constituent of interest (the tracer), u [m/s] is the cross-sectional average of the velocity, and D [m^2/s] is the longitudinal dispersion coefficient. The longitudinal direction variable is x[m], and t[s] is the time variable. A detailed derivation of the ADE for rivers is presented in Ref. 2, Section 1.8.4. The ADE equation serves as the starting point for many studies of dispersive flows and can be generalized in various directions (e.g., by adding a spatial dependence of u and D, or adding a first-order decay term, $-\beta C$). However, using average values over a fixed section of a river with similar characteristics (a 'reach') will suffice here.

The ADE is a linear wave equation; its linearity follows from the fact that dispersion is modeled linearly by Fick's Law, the same assumption that is made for a purely diffusive

process.[14] Dispersion combines both advection and diffusion, but in the case of a rapidly moving river, the advection process dominates, so molecular diffusion is ignored. The dimensionless Peclet number ($P_e = uL/D$) gauges the ratio of the rate of advective processes (uL) to diffusive processes (D); a very rough estimate yields $P_e > 20$ for the event flows in the upper reach of the Klamath River.

Recall that a Dirac function (more formally, a distribution[15]) can be viewed as the limit of a sequence of functions, with the typical example, a sequence of normalized Gaussian functions where

$$\lim_{x\to 0} \delta_\alpha(x) = \frac{1}{\sqrt{2\pi\alpha}} \exp\left(\frac{-x^2}{2\alpha}\right) \tag{2}$$

which, in the limit, illustrates the defining characteristics of the delta function

$$\delta(x) = \begin{cases} +\infty, & x = 0 \\ 0, & x \neq 0 \end{cases} \tag{3}$$

with

$$\int_{-\infty}^{+\infty} \delta(x)dx = 1, \text{ and } \int_{-\infty}^{+\infty} f(x)\delta(x)dx = f(0), \tag{4}$$

That is, a delta function picks out the value of a function $f(x)$ under the integral sign. The delta function is covered in many undergraduate physics courses to solve problems involving point masses and impulsive forces. Its properties are reviewed in Ref. 16, Section 1.5.

We use the delta function to mathematically define the addition of an instantaneous slug of turbidity at a point in the river.[17] Suppose this slug is introduced at position ξ in the river at time $t_0 = 0$, with total integrated turbidity (or sediment concentration) M: $C(\xi, 0) = M\delta(x_0, t–t_0)$. The delta function $\delta(x_0, t–t_0)$ ensures the concentration is localized at the exact position and time of application.

The solution to the one-dimensional advection-dispersion equation is commonly derived using a Fourier Transform (see Appendix A). Here we sketch a solution via a similarity transformation on an infinite domain:

$$-\infty < x < \infty, \ t > 0 \tag{5}$$

with a delta function source:

$$u(x, 0) = M\delta(x - x_0). \tag{6}$$

We note that the equation lacks a characteristic length and time scale for the fundamental solution. The spatial domain extends from $-\infty$ to ∞, means there are no physical boundaries to impose a specific length scale. The initial source condition is a Dirac delta function, which has no spatial extent or duration, so it does not set a characteristic length or time itself. The advection velocity u has units of length per time (L/T), and the dispersion coefficient D has units of length squared per time (L^2/T). The spatial scale of the spreading is related to $\sqrt{Dt}$, which changes with time. As time progresses, the spread becomes larger; there is no fixed characteristic length that the system settles on.

This absence of fixed scales means the problem is *scale-invariant* or exhibits *self-similarity*, allowing for the use of a similarity transformation. The problem's self-similarity suggests a solution dependent on a dimensionless similarity variable, commonly defined as

$$\eta = \frac{x - x_0 - ut}{\sqrt{4Dt}}. \tag{7}$$

Substituting a function of this form into the partial differential equation (PDE) reduces it to an ordinary differential equation (ODE) for the function of η.

Explicit integration of the ODE η for the 1D advection-dispersion with a delta function source on an infinite domain yields a moving Gaussian pulse:

$$C(x,t) = \frac{M}{\sqrt{4\pi Dt}} \exp\left(-\frac{(x - x_0 - ut)^2}{4Dt}\right) \tag{8}$$

This solution describes the concentration profile as a function of space and time. The center of the Gaussian pulse moves with the advection velocity u, and the pulse width increases due to dispersion, with a variance of $2Dt$.

As mentioned, we adopt the convention that the clock starts ($t_0 = 0$) when the delta function is dropped in the water. We will place our slug 'upstream' from our measurements stations, so note that this leads to the convention that our slug coordinate systems increase left to right (with the normal convention), but our slug moves right to left (Fig. 1), so time also increases as we go right to left — downstream. Ultimately, the convention for coordinates adopted here allows us to more easily match the solutions to the georeferenced river kilometers on a map. Practically, it means our spatial argument is written $x_0 - x$ in instead of the reverse.

After relabeling $x_0 = x_d$ (the delta function location) we arrive at the solution

$$f(x,t) = \frac{M}{\sqrt{4\pi D}} t^{-\frac{1}{2}} \exp\left(\frac{-(x_d - x - ut)^2}{4Dt}\right) \tag{9}$$

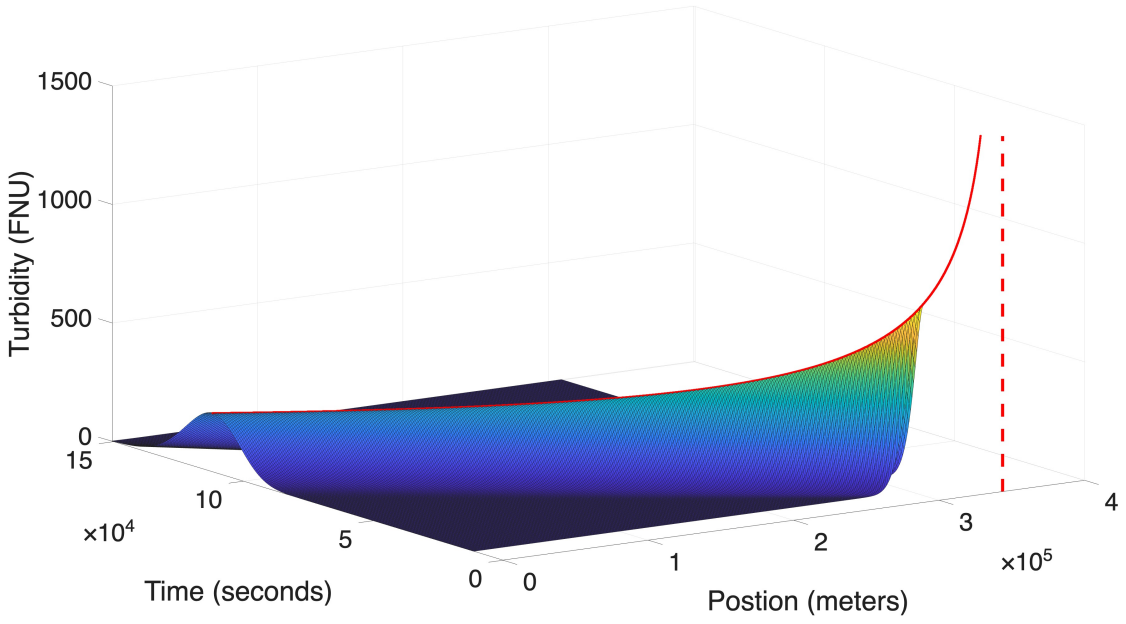

FIG. 5. Plot of Eq. 9 for the first delta function parameter values discussed in Sect. 4. The red curve is a trace of the peak value resulting from the evolution of a delta function indicated by the dashed line. Near the estuary (cross-section with river map position ≈ 0), the time profile is approximately Gaussian. By convention t_0 is defined by the position of the delta function, and time increases as the pulse moves downstream from Iron Gate to the estuary.

Figure 5 is a surface plot of Eq. 9. The dashed line indicates the position of the delta function, and the surface is a space-time plot of the resulting wave packet (slug) as it disperses downstream. Eq. 9 is called the 'fundamental' or 'principal solution' of the ADE equation because it is the kernel of the Green's Function, which refers to a general method for solving the ADE equation for a wide variety of boundary conditions by a convolution integral that exploits linear superposition.[18] If we hold t constant (i.e., 'fix t'), then the curve traced out by Eq. 9 is a Gaussian in the spatial dimension. The peak of the Gaussian occurs at

$$x_p(x) = x_d - ut. \tag{10}$$

However, turbidity is easier to measure if we fix 'x', that is, use a gauge at a fixed location. In that case we see an asymmetric curve like that in Fig. 6(a) as the slug passes. Differentiating with a natural log function, we find that the peak of a turbidity slug with a delta function at x_d passes by a gauge at position x_s at time[19]:

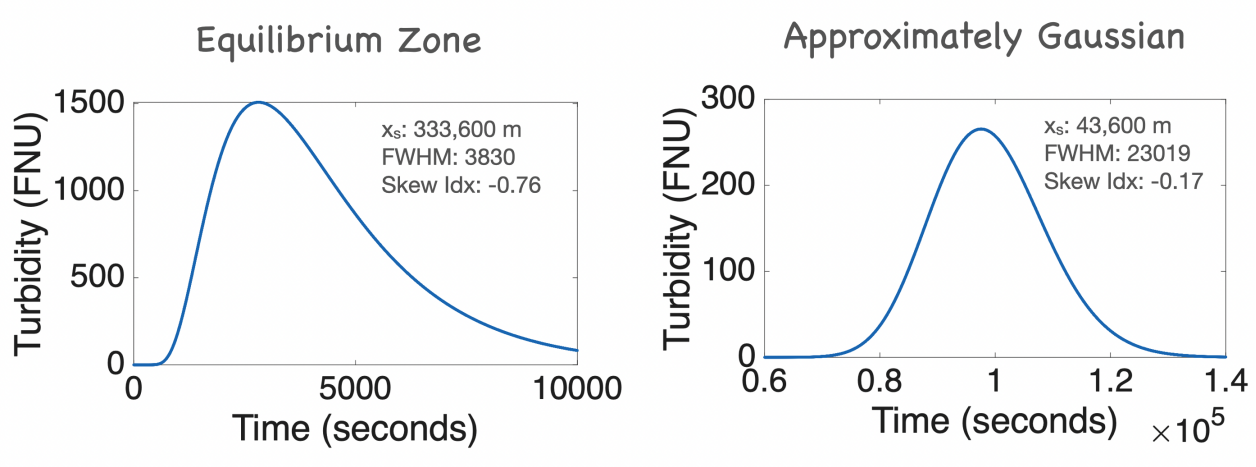

FIG. 6. Cross-sectional plots from Fig. 5. (a) The turbidity signal traced by a sensor at a fixed location $x_s = 333,600$ m. The plot is asymmetric, and its skewness decreases as the sensor location x_s moves downstream. This is the shape of a profile seen by sensors in the field at a fixed location in the intermediate field regime subject to a delta function pulse. (b) $x_s = 43,600$ m, as the slug moves far downstream its profile is approaching a symmetric Gaussian - the far field regime.

$$t_p(t) = \frac{1}{u^2}\left(\sqrt{D^2 + u^2(x_d - x_s)^2} - D\right). \tag{11}$$

The (red) curve at the top of the surface in Fig. 5 shows the trace of the peak defined by Eq. 9 in space (as the gauge station is moved) and time (as the slug passes the station at x_s). As time passes, we notice that the pulse becomes more symmetric and approaches the shape of a Gaussian (Fig. 6(b)). As the sensor position moves downstream the peak time approaches (from Eq. 9) $t_p \asymp (x_p - x_d)/u$ and using this in Eq. 9 we see the peak values decay as $x^{-1/2}$, that is,

$$C_p \asymp \frac{M}{\sqrt{4\pi D(x_d - x_p)/u}} \tag{12}$$

To describe the evolution of the turbidity slug, we can keep track of the spread of the pulse – the variance – as well as its asymmetry – its skewness. As a practical matter, we estimate the variance by computing the Full Width at Half Max (FWHM), and the skewness by

$$\gamma = \frac{(t_p - t_{trail}) - (t_{lead} - t_p)}{\text{FWHM}} \tag{13}$$

where t_{trail} and t_{lead} are the time differences between the arrival time of the peak and the arrival times of the half-max values that occur on the trailing and leading edges (Fig. 6(a)).

River scientists use the variance and the skewness to separate the evolution of the turbidity slug into three regimes. As illustrated in Fig. 7, plots of both the variance and skewness can be used to identify these three zones.[20,21]

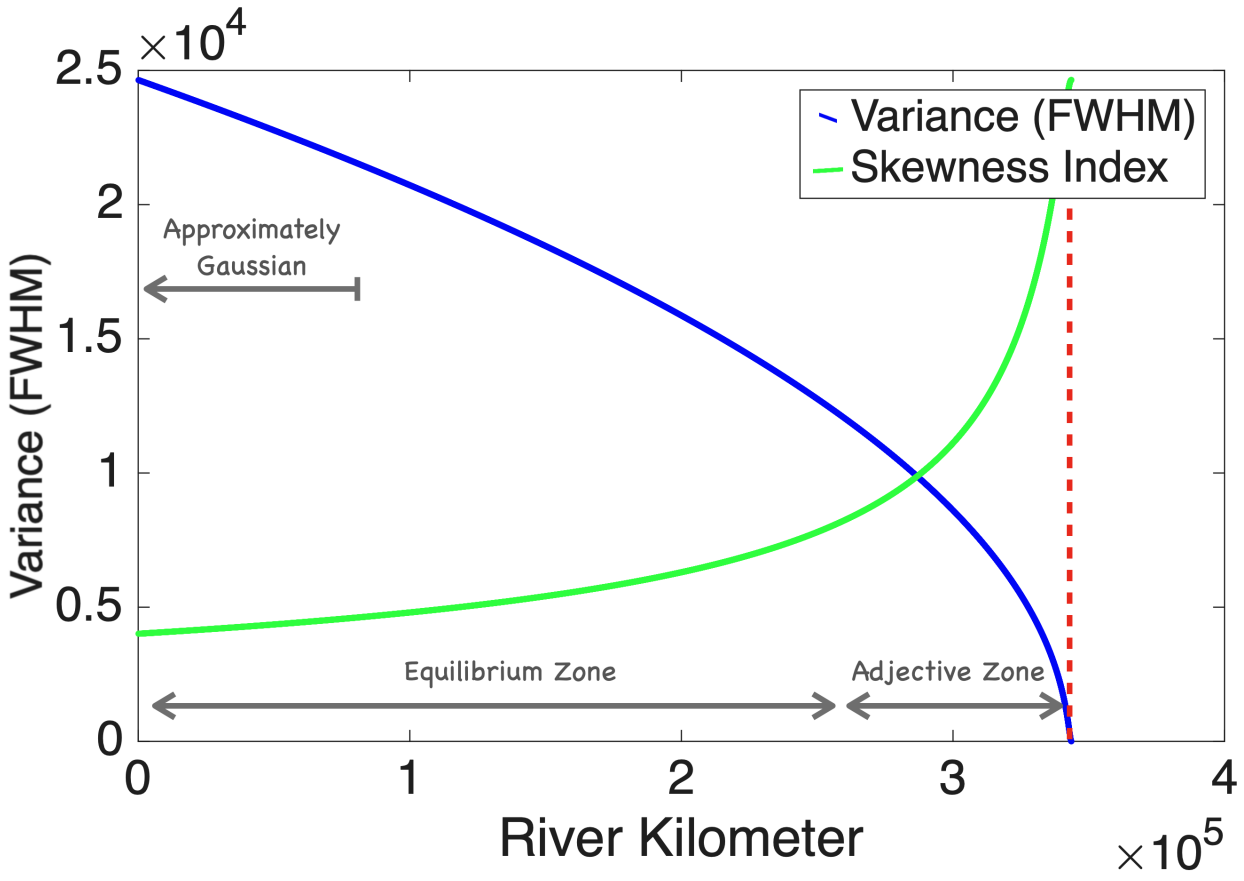

FIG. 7. When a (delta function) slug of sediment is placed in a river, the variance and skewness of the turbidity profiles can be used to distinguish three dynamical regimes. The 'advective zone' referes to the very near-field where there is still vertical and transverse mixing. An intermediate field – called the 'equilibrium zone' – references to when the the dispersion is primarily longitudinal and asymmetric (well mixed vertically and transversally). And a far-field where longitudinal dispersion is symmetric and Gaussian. For the plot, the skewness is normalized to the variance, and the dashed line indicates the location of the delta function. The pulse moves right to left – downstream, approaching river kilometer 0.

Initially, the skewness falls very rapidly; this is called the 'advective zone,' and is more properly characterized by a three-dimensional model. The most rapid process is vertical mixing, followed by transverse mixing across the river channel. The advective mixing regime

usually refers to these first two stages of mixing, which a one-dimensional model does not capture. Once the vertical and transverse directions are well mixed, the river is in the 'equilibrium zone' where the longitudinal model describes the evolution of dispersion in the direction of river flow. In the equilibrium regime, the variance increases approximately linearly, but the profile is still skewed. Quite a bit downstream, the third regime is indicated by a pulse response being very close to a Gaussian profile. The description here is purely qualitative but can be made more quantitative with a three-dimensional mixing model and the introduction of a dimensionless timescale.[22]

In Section 4, we describe how fitting the measured profile to the one generated by the principal solution (Eq. 9) allows us to specify the location of a delta function to approximate the flow. Essentially, the fitting procedure uses the nonlinearity of the leading edge of the profile to find optimal parameters. Of course, the downstream profile — due to dispersion — is determined by the complete initial upstream profile, which can be a complicated space-time surface for the initial shape of the turbidity. However, we will assume the steep leading edge of the profile is mainly determined by the initial part of the upstream profile,[23] which we model as a delta function — that is, the shape of the leading edge of the downstream profile is approximated by an upstream delta function. Mathematically, we are replacing the computation of the full convolution integral with an integral over one (or a few) delta functions to systematically model the shape of the downstream profile using the advection of the leading edge as our guide.

IV. ESTIMATION OF DELTA FUNCTION LOCATION

Figure 8 shows the signal of the turbidity (minus the baseflow turbidity of 92 FNU) as it passes the sensor at Iron Gate ($x_s = 309$ km). Note that the rising edge of the signal is sharp, and consists of 8 points (spaced at 15 minutes) showing a rise from its base flow value to its peak value $x_p = x_s$ at time $t_p = 22,675$ s and a peak turbidity value $C_p = 789$ FNU. We would like to place a delta function upstream of x_s so that, at least the leading edge of the measured signal, is close to that estimated by a delta function source.

Starting from Eq. 9, we want to determine an optimal set of parameters – M, D, x_d, u – so that the difference between the measured (leading edge) signal, $C_i = C(x_s, t_i)$ and that

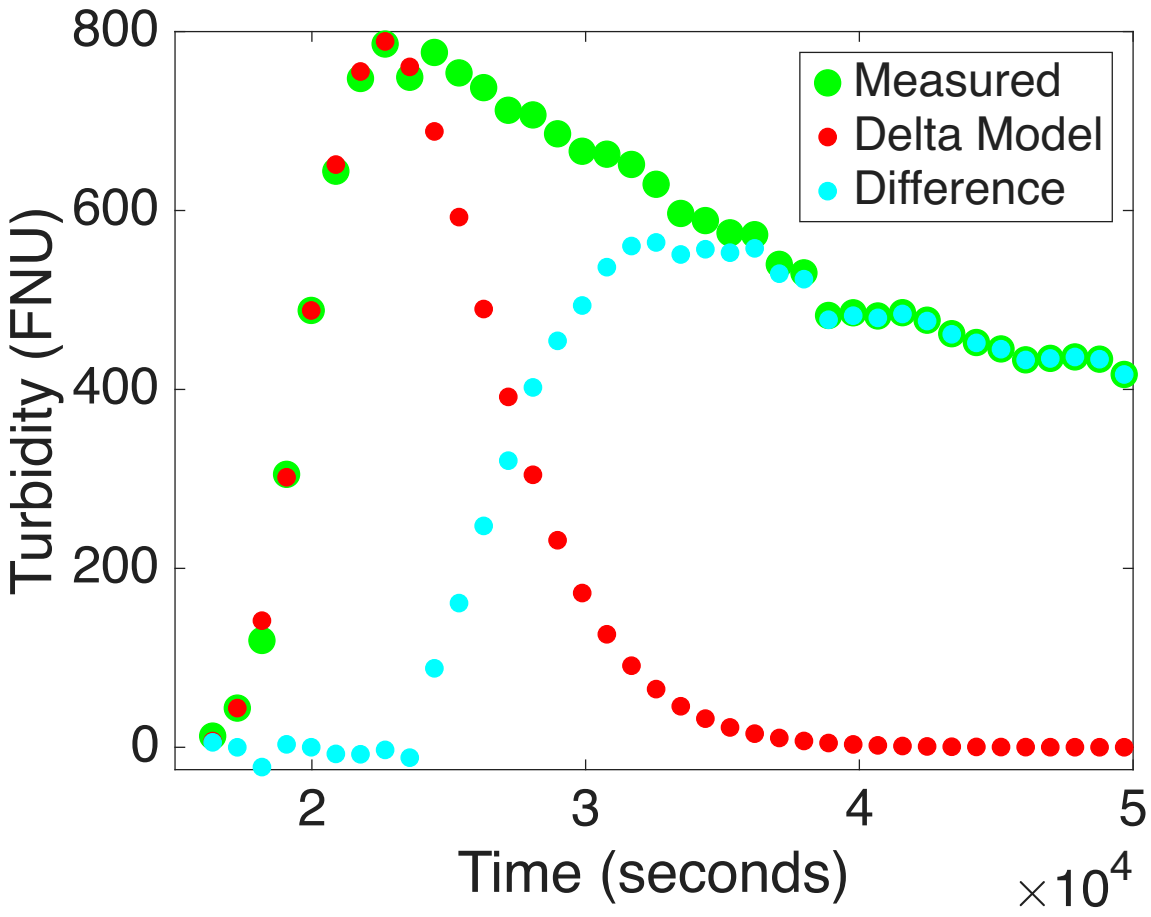

FIG. 8. Close-up of measured turbidity pulse (minus base flow) at Iron Gate, and a fit with the first delta function optimized to the leading edge (first 8 points).

predicted by the evolution of the delta function, $f_i = f(x_s, t_i)$ is minimized,

$$H_i(\cdot) = \frac{1}{N} \sum_{i}^{N} \sqrt{(C_i - f_i)^2}. \tag{14}$$

We perform this optimization with a number of simplifying assumptions. First, we use a fixed value of $u = 3.06$ m/s (the average value between Boyle and Iron Gate, see Table 1), and the optimization is performed only on the leading edge points – for the Iron Gate location this is the first eight points in Fig. 8. Further, once we pick an initial guess for the optimization parameters, – D, x_d – the value of M is also fixed using the peak value of the turbidity,

$$M = \sqrt{4\pi D}\; t_p^{\frac{1}{2}} \left[1/\exp\left(\frac{-(x_d - x_s - u t_p)^2}{4 D t_p} \right) \right] \tag{15}$$

It is common practice to use a local search method when finding optimization parameters, however, in this instance, the evaluation of the functions are simple enough so that under a reasonable range of parameters (e.g. $x_d \in [309, 385]$ km, $D \in [1, 5000]$ m^2/s) we can evaluate a full grid of points and search for a global optimum. Note that the 'Dispersion Constant' estimated with this method, like the delta function itself, is a fiction – a numerical tool – that, at best, is perhaps a very rough upper bound for what an experimental tracer measurement might observe. This is due, in part, to the fact that the delta function model is operating under a 'advective' regime for much of the flow (the maxima of the delta function solution very rapidly decrease as it heads downstream), whereas the actual flow in the same spatial domain is undergoing a very different behavior.

A surface plot of the inverse of the optimization function (Eq. 14) is presented in Fig. 9 for different combinations of D and x_d. A unique global maximum is occurs at $D \approx 4593$ m^2/s and $x_d \approx 343600$ m. The occurrence of a unique global maximum in the parameter regime directly follows from the choice of a fixed value for the velocity, $u = 3.06$ m/s – because the rising edge is sharp (closely spaced in time) the arrival time of all the leading edge points are close, and this in turn sets the location of x_d relative to x_s; the selection of D provides a fine a tuning for the final fit. A comparison of the delta function fit to the leading edge of the pulse at Iron Gate is shown in Fig. 8. On the first eight points of the data, the estimation of pulse is excellent, the mean error is ≈ 6 FNU. As expected, after the 9th point the error systematically rises.

Is there anything interesting at the $x_d \approx 343$ km? Fig. 1 shows that x_d is at the approximate location of Copco Dam 1 – and at the end of the steep gradient between Boyle Dam and Copco Dam. We hypothesize that the energetic flow in this section of the river ($u_{avg} = 7.78$ m/s) causes the resuspension of sediments that strengthens the turbidity pulse in this section. This hypothesis is supported by the remote sensing which shows regions, such as the location of the J. C. Boyle reservoir, that are rich with exposed sediments in early 2025 (see Fig. 10). Part of the restoration efforts is to stabilize these sediments with native vegetation. Mathematically at least, the use of a delta function allows us to summarize the downstream effects of this pulse with an estimation of both its arrival time, initial rise, and sediment dispersion.

To approximate the pulse beyond the leading edge, we can peel off the first delta function from the measured data and fit the leading edge of the remaining turbidity signal to a second

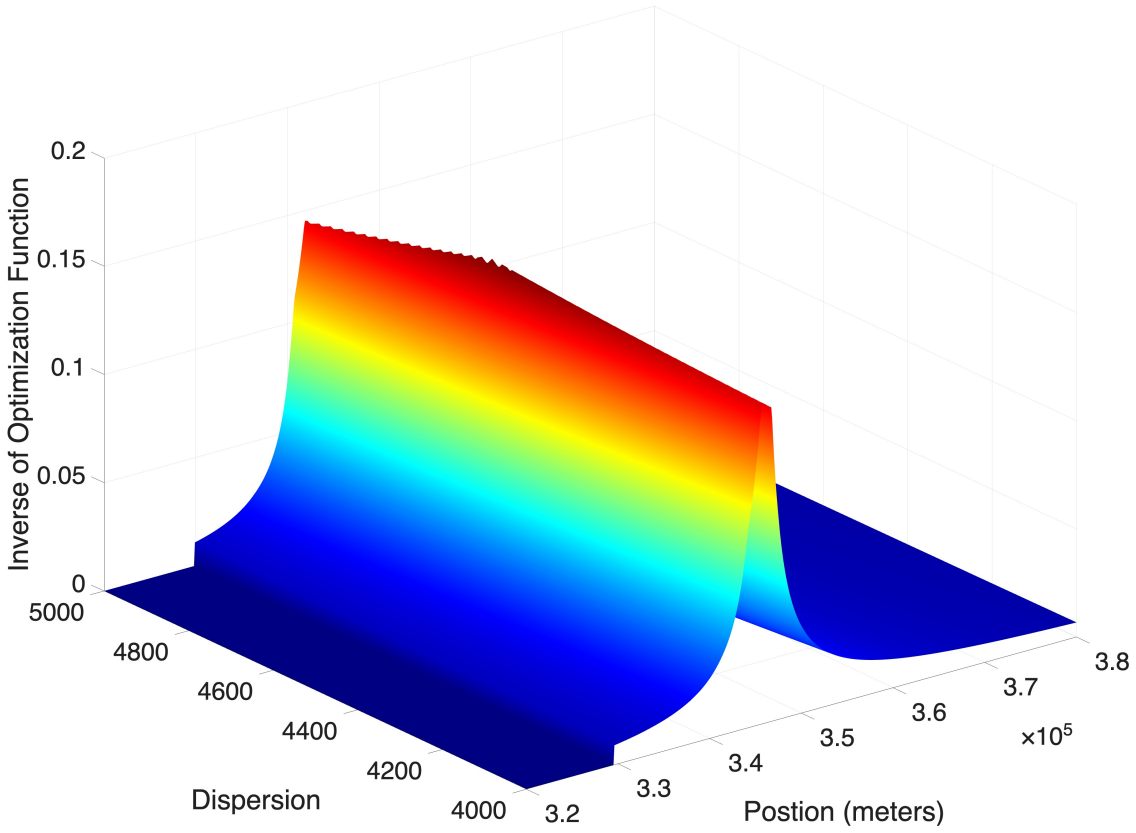

FIG. 9. Inverse of optimization function used to identify flow parameters $D = 4,593$ m^2/s and $x_d = 343,600$ m, the dispersion and location of the upstream delta function to match the leading edge of the downstream turbidity signal at Iron Gate. A global optimum is visible in about the center of the plot which determines the optimal parameter values.

delta function. Figure 11 shows the resulting fit (with an average error of 9 FNU) of the lead edge (first 12 points) with $D = 18060$ m^2/s and $x_d = 386200$ m – which happens to be the location of Keno Dam, the original release point of the pulse. The resulting fit of the turbidity pulse from the sum of the first and second delta functions is shown in Fig. 12. The agreement between the minimal two delta model, and the measurement data, is very good for the first 5 hours (20 points $\times$ 0.25 hours/pts).

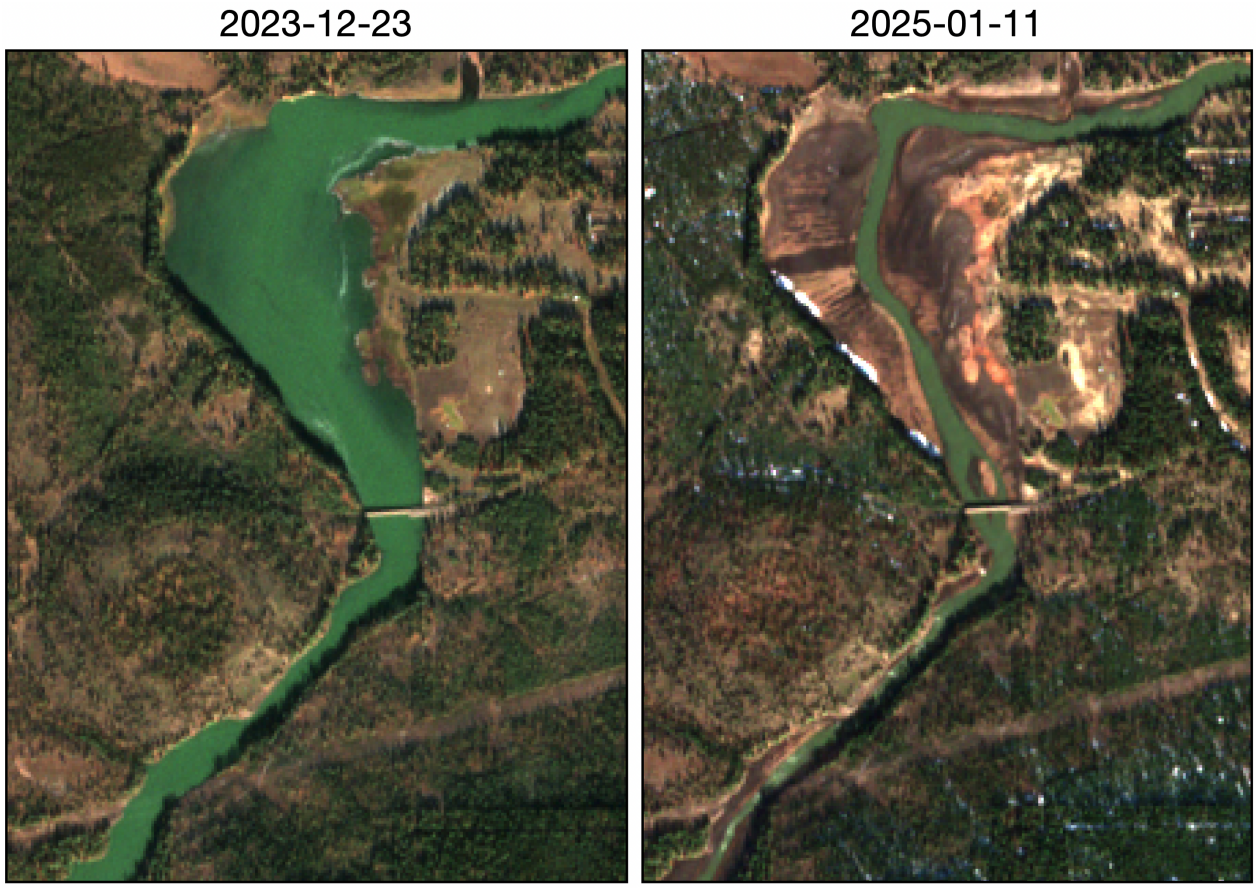

FIG. 10. Sentinel-2 images showing (left) pre-dam removal water in the J. C. Boyle Reservoir (23 December 2023), and (right) exposed sediments after dam removal in early 2025 (11 January 2025).

V. CONCLUDING REMARKS

The examination of a data set following a pulse of turbidity down the Klamath River on 27 November 2025 provides a useful illustration of a fundamental physical flow model, the Advection-Dispersion Equation, and its application to sediment transport in rivers. The basic theory and data analysis are accessible to undergraduate science students, and provides an environmentally relevant application of the utility of linear wave theory.

In addition, a waveform approximation procedure is described, which might be called a 'skewed-dynamic' radial-basis function method,[24] to compactly represent the downstream leading edge (flooding stage) of the turbidity pulse. The next step would be the systematic prediction of these pulses based on a convolution integral, or difference/differential model (e.g. a Kalman Filter), and river engineering methods are currently being developed in that

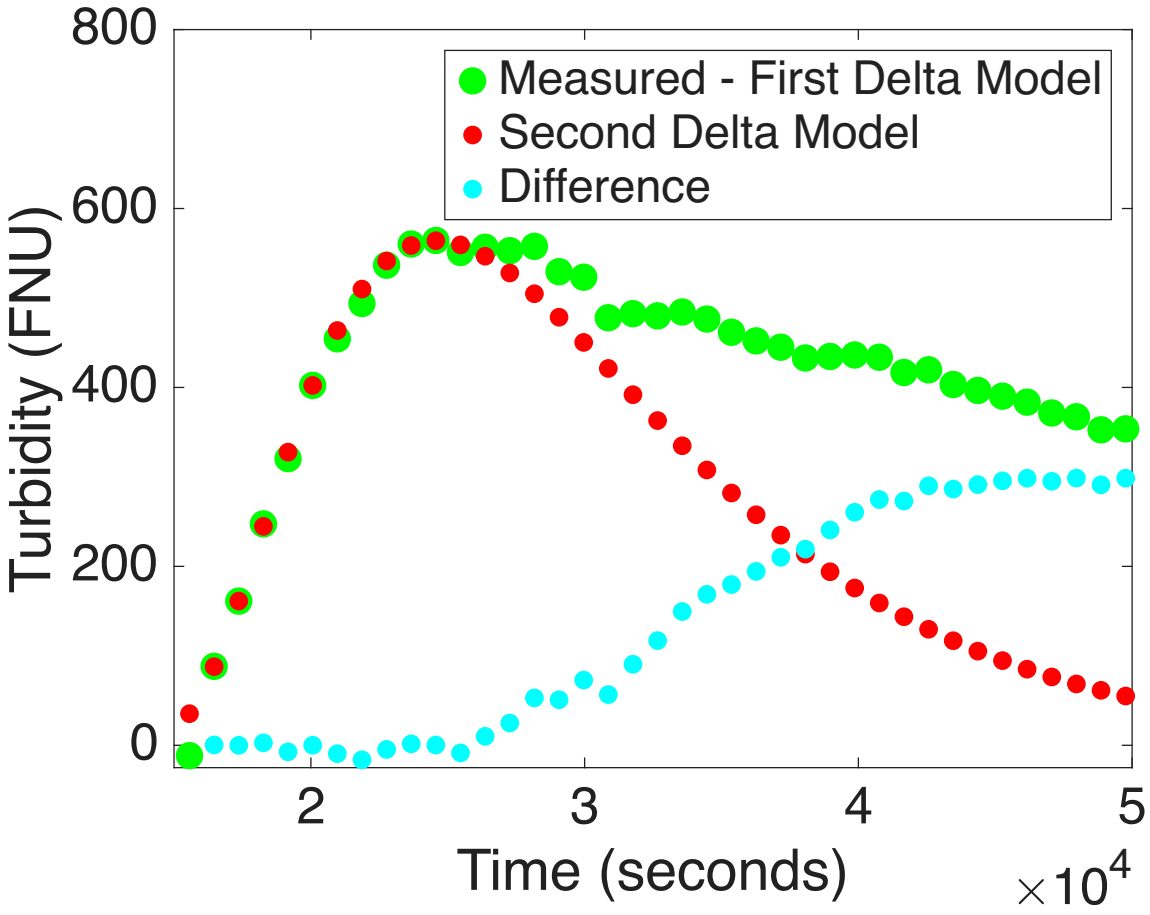

FIG. 11. Close-up of measured turbidity at Iron Gate minus the first delta function. A fit with the second delta function optimized to the leading edge (first 12 points).

direction, not just for a single river reach but also for river networks.[25–27]

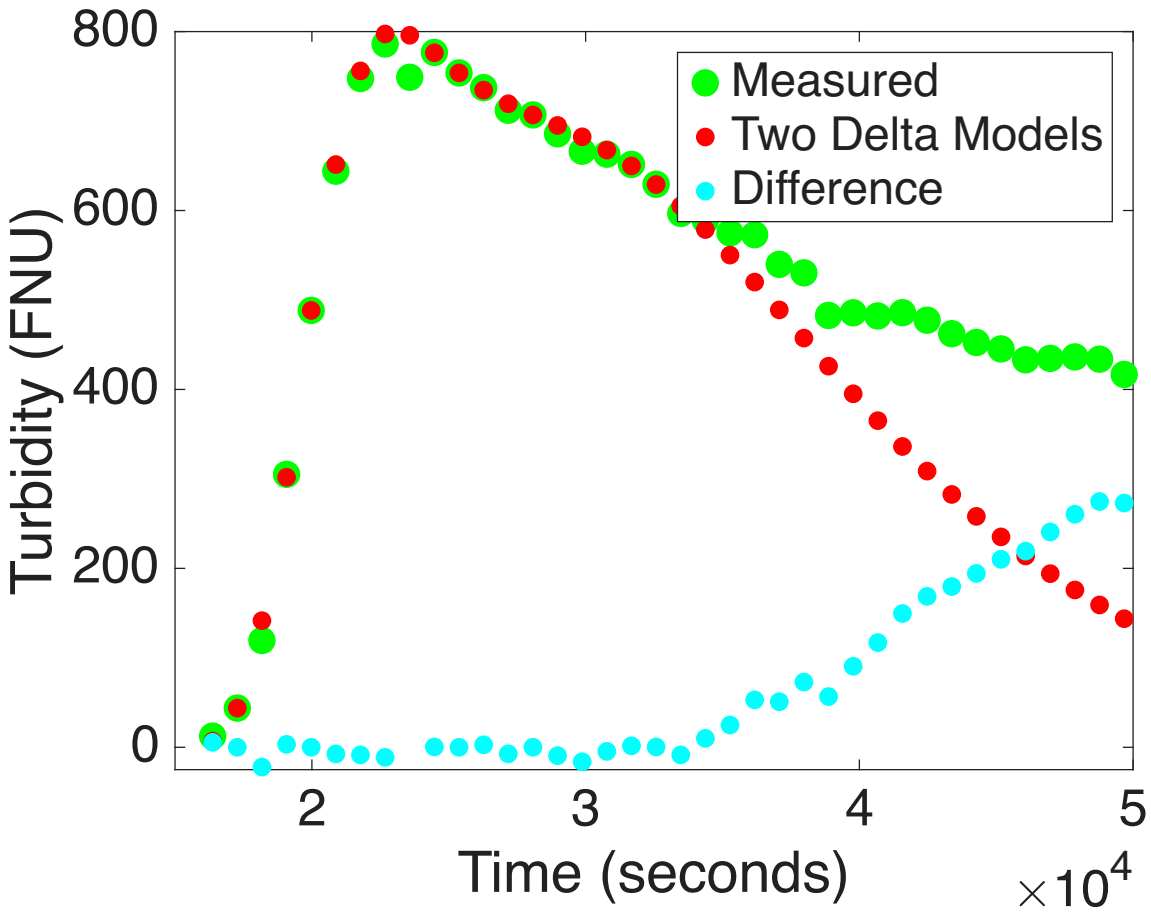

FIG. 12. The difference between the measured turbidity at Iron Gate and the sum of the first and second delta functions. The agreement is very good over the flooding state, the first 5 hours (20 points).

APPENDIX A: DERIVATION OF THE FUNDAMENTAL SOLUTION TO THE 1D ADVECTION-DISPERSION EQUATION USING THE FOURIER TRANSFORM

The one-dimensional advection-dispersion equation (ADE) is a classic PDE used to describe the transport of a solute in a fluid, accounting for both advection and dispersion. The equation for a concentration $C(x,t)$ is given by:

$$\frac{\partial C}{\partial t} = D\frac{\partial^2 C}{\partial x^2} - u\frac{\partial C}{\partial x} \tag{A-1}$$

where D is the dispersion coefficient and u is the advective velocity. We seek the fundamental solution, which corresponds to the initial condition of a Dirac delta function:

$$C(x,0) = M\delta(x) \tag{A-2}$$

where M is the total mass of the solute injected at $x = 0$ at $t = 0$.

We use the Fourier transform method to solve the PDE. The Fourier transform of $C(x,t)$ with respect to x is defined as:

$$\hat{C}(k,t) = \mathcal{F}\{C(x,t)\} = \int_{-\infty}^{\infty} C(x,t)e^{-ikx}dx \tag{A-3}$$

Applying the Fourier transform to the ADE, we use the properties of the transform for derivatives:

$$\mathcal{F}\left\{\frac{\partial C}{\partial t}\right\} = \frac{\partial \hat{C}}{\partial t}$$
$$\mathcal{F}\left\{\frac{\partial C}{\partial x}\right\} = ik\hat{C}$$
$$\mathcal{F}\left\{\frac{\partial^2 C}{\partial x^2}\right\} = (ik)^2\hat{C} = -k^2\hat{C}$$

Substituting these into the transformed equation, we get an ODE in time:

$$\frac{\partial \hat{C}}{\partial t} = D(-k^2)\hat{C} - u(ik)\hat{C} = -(Dk^2 + iku)\hat{C} \tag{A-4}$$

The ODE in (A-4) is first-order and linear, with a solution of the form:

$$\hat{C}(k,t) = A(k)e^{-(Dk^2+iku)t} \tag{A-5}$$

The initial condition in the Fourier domain is found by transforming the initial condition $C(x,0) = M\delta(x)$:

$$\hat{C}(k,0) = \int_{-\infty}^{\infty} M\delta(x)e^{-ikx}dx = Me^{-ik(0)} = M \tag{A-6}$$

Using this initial condition, we find $A(k) = M$. Thus, the solution in the Fourier domain is:

$$\hat{C}(k,t) = Me^{-(Dk^2+iku)t} = Me^{-Dk^2t}e^{-ikut} \tag{A-7}$$

To find the solution $C(x,t)$ in the physical domain, we apply the inverse Fourier transform:

$$C(x,t) = \mathcal{F}^{-1}\{\hat{C}(k,t)\} = \frac{1}{2\pi}\int_{-\infty}^{\infty} \hat{C}(k,t)e^{ikx}dk \tag{A-8}$$

Substituting the expression for $\hat{C}(k,t)$:

$$C(x,t) = \frac{M}{2\pi}\int_{-\infty}^{\infty} e^{-Dk^2t}e^{-ikut}e^{ikx}dk = \frac{M}{2\pi}\int_{-\infty}^{\infty} e^{-Dk^2t+ik(x-ut)}dk \tag{A-9}$$

We can complete the square in the exponent with respect to k. Let $\xi = x-ut$. The exponent is $-Dtk^2 + i\xi k$.

$$\begin{aligned}
-Dtk^2 + i\xi k &= -Dt\left(k^2 - \frac{i\xi}{Dt}k\right) \\
&= -Dt\left(k^2 - \frac{i\xi}{Dt}k + \left(\frac{i\xi}{2Dt}\right)^2 - \left(\frac{i\xi}{2Dt}\right)^2\right) \\
&= -Dt\left(\left(k - \frac{i\xi}{2Dt}\right)^2 - \frac{\xi^2}{4D^2t^2}\right) \\
&= -Dt\left(k - \frac{i\xi}{2Dt}\right)^2 + \frac{\xi^2}{4Dt}
\end{aligned}$$

The integral becomes:

$$C(x,t) = \frac{M}{2\pi}e^{\frac{\xi^2}{4Dt}}\int_{-\infty}^{\infty} e^{-Dt\left(k-\frac{i\xi}{2Dt}\right)^2}dk \tag{A-10}$$

We use a change of variables, $u = k - \frac{i\xi}{2Dt}$, so $dk = du$. The integration path in the complex plane remains on a line parallel to the real axis. By Cauchy's integral theorem, this integral is equal to the standard Gaussian integral along the real axis $\int_{-\infty}^{\infty} e^{-Dtu^2}du = \sqrt{\frac{\pi}{Dt}}$.

$$C(x,t) = \frac{M}{2\pi}e^{\frac{\xi^2}{4Dt}}\sqrt{\frac{\pi}{Dt}} = \frac{M}{\sqrt{4\pi Dt}}e^{-\frac{(x-ut)^2}{4Dt}} \tag{A-11}$$

The fundamental solution to the one-dimensional advection-dispersion equation is a Gaussian function that disperses over time and whose center moves with the advective velocity u. The solution is:

$$C(x,t) = \frac{M}{\sqrt{4\pi Dt}}\exp\left(-\frac{(x-ut)^2}{4Dt}\right) \tag{A-12}$$

This solution is a classic result in fluid dynamics and chemical engineering and is widely used to model contaminant transport.

ACKNOWLEDGEMENTS

To be added after review.

* nick@gybe.eco

[1] Amy Bowers Cordalis, *The Water Remembers: My Indigenous Family's Fight to Save a River and a Way of Life* (Little, Brown, & Company, New York, 2025).

[2] J. C. Rutherford, *River Mixing* (Wiley, New York, 1994).

[3] C. J. Legleiter, Carl J., B. Sansom, and R. Jacobson, "Remote sensing of visible dye concentrations during a tracer experiment on a large, turbid river," Water Resources Research **58** (4) Article ID: e2021WR031396 (2022).

[4] Model archive summary for suspended-sediment concentration at station 11516530, Klamath River below Iron Gate Dam, California, WY 2019-2023, <https://www.usgs.gov/data/model-archive-summary-suspended-sediment-concentration-station-11516530-klamath-river-below>.

[5] N. Tufillaro, P. Grötsch, I. Lalović, I., S. Moitié, L. Zeitlin, L., & O. Zurita, "Monitoring water quality in the lower Kansas River using remote sensing," River, **3** (3), 284–303 (2024).

[6] Data portal for Karuk Tribe Water Quality Gauges on the Klamath, <https://waterquality.karuk.us/>

[7] USGS Klamath River Basin Water-Quality Mapper <https://or.water.usgs.gov/projs_dir/klamath_wq_mapper/>

[8] T. Matos, M.S. Martins, R. Henriques, L.M. Goncalves, "A review of methods and instruments to monitor turbidity and suspended sediment concentration," Journal of Water Process Engineering, **64**, 105624 (2024)

[9] The remote sensing images are generated from L1C Sentinel-2 files downloaded from ESA's Copernicus Hub and processed with Acolite to RGB imagery. Q. Vanhellemont, "Adaptation of the dark spectrum fitting atmospheric correction for aquatic applications of the Landsat and Sentinel-2 archives," Remote Sensing of Environment, **225**, 175-192 (2019).

[10] T. Kailath, *Linear systems* (Prentice-Hall, New York, 1980.)

[11] H. B. Fisher, "Dispersion predictions in natural streams." Journal of the Sanitary Engineering Division **94**(5), 927-943 (1968).

[12] "Sediment routing model for the Klamath River," in preparation.

[13] J. von Neumann, *Mathematische Grundlagen der Quantenmechanik* (Springer, Berlin, 1932).

[14] J. Crank, *The mathematics of diffusion (2nd ed.).* (Oxford University Press, Oxford, 1979).

[15] D. J. Griffiths and S. Walborn, "Dirac deltas and discontinuous functions," Am. J. Phys. **67** (5), 446–447 (1999)

[16] D. J. Griffiths, *Introduction to Electrodynamics, Fifth edition.* (Cambridge University Press, Cambridge, 2024).

[17] The slug is actually a sediment concentration, while turbidity is an optical signature of sediment backscatter. Thus, calling it a slug of turbidity is probably a misnomer, but we use this language here for simplicity and treat turbidity as if it is normalizable and conserved, similar to sediment concentration.

[18] W. A. Jury and K. Roth, *Transfer functions and solute movement through soil: theory and applications* (Birkhäuser Verlag, Berlin, 1990)

[19] P. A. Krenkel, "Waste Dispersion Characteristics of Streams Using Turbulent Diffusion Phenomenon," Journal of Water and Pollution Control **34**(12),1203-1212 (1962)

[20] K. M. Pace, D. D. Tullos, C. Walter, S. Lancaster,& C. Segura, "Sediment pulse behaviour following dam removal in gravel-bed rivers." River research and applications, **33** (1), 102-112 (2017).

[21] It is more common in river engineering to track the evolution of a pulse by its statistical moments rather than its peak, see Ref. 20. The 1st and 2nd moments computed from the pulse of Eq. 9 are ($\eta = (x_d - x)$): $\bar{t} = (\eta/u) + (2D/u^2)$ and $\sigma^2 = (2D\eta)/u^3) + (8D^2/u^4)$.

[22] P. J. Sullivan, "Longitudinal dispersion within a two-dimensional turbulent shear flow," J. Fluid Mech., **49**(3), 551-576 (1971)

[23] P. C. Chatwin, "On the interpretation of some longitudinal dispersion experiments," J. Fluid Mech., **48**(4), 689-702 (1971)

[24] M. Aminian and M. Kirby, "Reduced Order Modeling with Skew-Radial Basis Functions for Time Series Prediction," Eng. Proc. **39**, 93 (2023).

[25] M. Bartos and B. Kerkez, "Pipedream: An interactive digital twin model for natural and urban drainage systems," Environmental Modelling & Software, **144**, 105120 (2021).

[26] M. Shilsar, M. Mazaheri, and J. Samani, "A semi-analytical solution for one-dimensional pollutant transport equation in different types of river networks," Journal of Hydrology, **619**, 129287 (2023).

[27] A. Haddadchi, C. W. Rose, "An advection-dispersion model for routing suspended sediment down the river network," Environmental Modelling & Software, **188**, 106417 (2025).